FP7-600716

Whole-Body Compliant Dynamical Contacts in Cognitive Humanoids

Year 4
Fourth year project objectives report

Editor(s)	CoDyCo Consortium
Responsible Partner	IIT
Affiliations	IIT, TUD, UPMC, UB, JSI.
Status-Version:	Draft-1.0
Date:	Apr. 28, 2017
EC Distribution:	Consortium
Project Number:	600716
Project Title:	Whole-Body Compliant Dynamical Contacts in Cognitive Humanoids

Title of Report:	Fourth year project objectives report
Date of delivery to the EC:	28/04/2017

Workpackage responsible for the Report	All work packages
Editor(s):	Francesco Nori, Vincent Padois, Jan Peters, Jan Babic, Michael Mistry
Contributor(s):	Entire CoDyCo consortium
Reviewer(s):	reviewers
Approved by:	All Partners

Table of Contents

Index of Figures

3.2 Project objectives for the period

3.2.1 Overview

The specificity of CoDyCo relies on the fact that the progress beyond the state of the art is guided by the yearly implementation on the iCub humanoid. Within this context, iCub is a peculiar platform being the only humanoid integrating whole-body distributed force and tactile sensors. In this sense CoDyCo fourth year specific objectives were to design and implement the control of whole-body posture during physical human robot interaction. Other long term objectives involve setting up the necessary infrastructure (human experimental protocols, software infrastructure, learning and control specifications) for leveraging the activities in previous years.

Task	IIT	TUD	UPMC	UB	JSI	INRIA	
WP1	0.00	1.00	-	2.18	2.00	2.96	8.14
WP2	-	1	1.20	13.88	21.69	0.52	38.29
WP3	-	9.65	8.79	1.63	2.00	4.03	26.10
WP4	9.79	12	0.74	1.68	3.00	3.30	30.51
WP5	13.06	2	0.14	1.44	-	0.52	17.16
WP6	1.51	1	0.19	-	0.44	-	3.14
WP7	1.00	-	0.11	-	-	-	1.11
	25.36	26.65	11.17	20.81	29.13	11.33	**123.45**

3.2.1.1 WP1: toolbox for computing and controlling dynamics of whole-body movements with contacts (UB)

- The overall goal of this work package is to ...
- The expected outcomes for year 1 were ...

3.2.1.2 WP2: understanding and modelling human whole-body behaviours in physical interaction (JSI) There were two main objectives within WP2 for the fourth year of the project: (i) to continue the work on unpredictable perturbations of human whole-body behaviour (Task 2.3) and (ii) to continue to study the factors involved in generalization and adaptation of skills learnt in contact with the compliant environment (Task 2.4).

3.2.1.3 WP3: control and optimization of whole-body motion in contact (UPMC)

- The overall goal of this work package is to ...
- The expected outcomes for year 1 were ...

3.2.1.4 WP4: adaptation, Generalization and Improvement of Compliant Control and Tasks with Contacts (TUD)

- The overall goal of this work package is to ...
- The expected outcomes for year 1 were ...

3.2.1.5 WP5: systems integration, standardization and evaluation on the iCub robot (IIT) The fourth year main objective for WP5 was the implementation of a validation scenario consisting of the assisted standing up motion.

3.2.1.6 WP6: management (IIT) The fourth year management was primarily dedicated to the project concluding activities.

3.2.1.7 WP7: dissemination and Exploitation (IIT) The main dissemination objectives for the CoDyCo fourth year were the publication of scientific papers and videos.

3.3 Work progress and achievements during the period

3.3.1 Progress overview and contribution to the research field

All the CoDyCo fourth year objectives have been attained. Here is a list of the CoDyCo fourth year achievements.

-
-
-

3.3.2 Work packages progress

WP1: toolbox for computing and controlling dynamics of whole-body movements with contacts (UB) WP1 objectives were achieved for the fourth year. In summary, the main accomplishments and impacts for the research community are as follows:

-
-
-
-

WP2: understanding and modelling human whole-body behaviours in physical interaction (JSI) After the fourth year of project, WP2 objectives were achieved for the fourth year. In summary, the main accomplishments and impacts for the research community are as follows:

-
-
-
-

WP3: control and optimization of whole-body motion in contact (UPMC) After the fourth year of project, WP3 objectives were achieved for the fourth year. In summary, the main accomplishments and impacts for the research community are as follows:

-
-
-
-

WP4: adaptation, generalization and improvement of compliant control and tasks with contacts (TUD) After the fourth year of project, WP4 objectives were achieved for the fourth year. In summary, the main accomplishments and impacts for the research community are as follows:

-
-
-
-

WP5: systems integration, standardization and evaluation on the iCub robot (IIT) The fourth year WP5 activities have concentrated on the fourth year validation scenario. A complete description of the scenario can be found in "D5.4 Validation scenario 4: learning how to stand up with the help of a human caregiver.." which discusses the technical implementation of the fourth year validation scenario (see `https://github.com/robotology-playground/codyco-deliverables/tree/master/D5.4/pdf`). With respect to the state of the art the work progress represents an implementation of well established torques controlled whole-body control strategies. The integration of tactile feedback within the whole-body controller is a peculiarity of the implemented CoDyCo validation scenario and therefore represent a step forward with respect to the current state of the art. At the moment of writing the current deliverable the iCub tactile sensors cover the feet, the torso, the arms and the hands and the implemented validation scenario accounts for contacts at the hands and feet.

WP6: management (IIT) The CoDyCo project management was concluded successfully. Management activities included the definition of an amendment procedure smoothly organized by the consortium and the project officer. The software repository (`https://github.com/robotology/codyco`) was consolidated on github (`https://github.com`).

WP7: dissemination and exploitation (IIT) Within WP7, CoDyCo fourth year achievement include: dissemination at relevant academic and industrial events; realization of a CoDyCo experiment database to disseminate robot and humans datasets.

3.3.2.1 Work package 1 progress

3.3.2.1.1 Software architecture design and evaluation of available open-source software pertinent to the scope of the project. (T1.1) The explicit goal of T1.1 for the fourth year was to ...

We achieved the following results ...

3.3.2.1.2 Simulator for whole-body motion with contacts (T1.2) The explicit goal of T1.2 for the fourth year was to ...

We achieved the following results ...

3.3.2.1.3 Control library for flexible specification of task space dynamics of floating base manipulators. (T1.3) The explicit goal of T1.3 for the fourth year was to ...

We achieved the following results ...

3.3.2.1.4 System dynamics estimation software. Extension to environmental compliance estimation (T1.4) The explicit goal of T1.4 for the fourth year was to ...

We achieved the following results ...

3.3.2.1.5 Extension and enhancement of the iDyn library. (T1.5) The explicit goal of T1.5 for the fourth year was to ...

We achieved the following results ...

Resources Overall, the use of resources within WP1 was in accordance to the plans.

WP1 person months	IIT	TUD	UPMC	UB	JSI	INRIA
Year 1	8.67	1.00	3.29	0.51	2.00	-
Year 2	3.00	3.00	0.47	2.29	-	-
Year 3	-	1.00	-	2.18	2.00	2.96
Year 4	?	?	?	?	?	?
Partial	?	?	?	?	?	?
Overall	12.00	9.00	6.00	15.00	6.00	5.00

Deviations from workplan Overall the project is aligned with the plan. UB has been organised next year activity to fully exploit the remaining person months.

3.3.2.2 Work package 2 progress

CoM dynamic manipulability as a tool to study, analyze and measure physical abilities of humans and robots As part of T2.2 and also T2.3, UB continued on improving CoM dynamic manipulability as a tool to study, analyze and measure physical abilities of humans and robots. First, the equation for the CoM manipulability ellipsoid was modified to decompose the effect of velocity and gravity related accelerations from the configuration dependent parts. Then, two different choices for the weighting matrix were introduced in order to evaluate the physical ability to accelerate the CoM with certain limits at the joint torques or joint accelerations.

Progress

Assuming unit weighted norm of actuated joint torques as

$$\boldsymbol{\tau}^T \mathbf{W}_\tau \boldsymbol{\tau} = 1\,, \tag{1}$$

the modified inequality of the CoM manipulability ellipsoid is

$$0 \leq (\ddot{\mathbf{c}} - \ddot{\mathbf{c}}_{vg})^T (\mathbf{J}_\tau \mathbf{W}_\tau^{-1} \mathbf{J}_\tau^T)^{-1} (\ddot{\mathbf{c}} - \ddot{\mathbf{c}}_{vg}) \leq 1\,, \tag{2}$$

where $\mathbf{W}_\tau$ is the weighting matrix and $\ddot{\mathbf{c}}$ is the CoM acceleration as

$$\ddot{\mathbf{c}} = \mathbf{J}_\tau \boldsymbol{\tau} + \ddot{\mathbf{c}}_{vg}\,, \tag{3}$$

$\mathbf{J}_\tau$ is a Jacobian that maps joint torques to the CoM acceleration and $\ddot{\mathbf{c}}_{vg}$ is the velocity and gravity dependent part of the CoM acceleration. The center of this ellipsoid is $\ddot{\mathbf{c}}_{vg}$ and its radii and orientation can be determined by the eigenvectors and eigenvalues of matrix $(\mathbf{J}_\tau \mathbf{W}_\tau^{-1} \mathbf{J}_\tau^T)$. Therefore, the size and shape of ellipsoid is configuration dependent only. Velocity and gravity only alter the location of the ellipsoid within the space of the CoM acceleration.

Different choices can be used for $\mathbf{W}_\tau$ based on the application. Here, we discuss two reasonable choices that can be used for general purposes.

First Choice: Torque Limits

Our first proposed reasonable choice for $\mathbf{W}_\tau$ is

$$\mathbf{W}_\tau^{-1} = \mathrm{diag}([k\boldsymbol{\tau}_{1_{max}}^2, k\boldsymbol{\tau}_{2_{max}}^2, \ldots, k\boldsymbol{\tau}_{k_{max}}^2])\,, \tag{4}$$

where $\boldsymbol{\tau}_{i_{max}}$ is the saturation limit at the ith joint ($i = 1, 2, ..., k$) and $|\boldsymbol{\tau}_i| \leq \boldsymbol{\tau}_{i_{max}}$. By using this weighting matrix, (1) will become

$$\frac{\boldsymbol{\tau}_1^2}{\boldsymbol{\tau}_{1_{max}}^2} + \frac{\boldsymbol{\tau}_2^2}{\boldsymbol{\tau}_{2_{max}}^2} + \cdots + \frac{\boldsymbol{\tau}_k^2}{\boldsymbol{\tau}_{k_{max}}^2} = k\,. \tag{5}$$

Since the ellipsoid in (5) accommodates all combinations of available joint torques (i.e. $\boldsymbol{\tau}_i^2/\boldsymbol{\tau}_{i_{max}}^2 \leq 1$), the outcome ellipsoid in (2) will include all achievable accelerations of the CoM.

In order to verify our choice of $\mathbf{W}_\tau$ and to illustrate the relationship between manipulability ellipsoid (ellipse in 2D) by using (4) and achievable CoM accelerations due to torque limits, we plot ellipses for four different planar robots at zero velocity and gravity (i.e. $\ddot{\mathbf{c}}_{vg} = 0$), assuming arbitrary torque limits. These four robots consist of (i) four, (ii) five, (iii) seven and

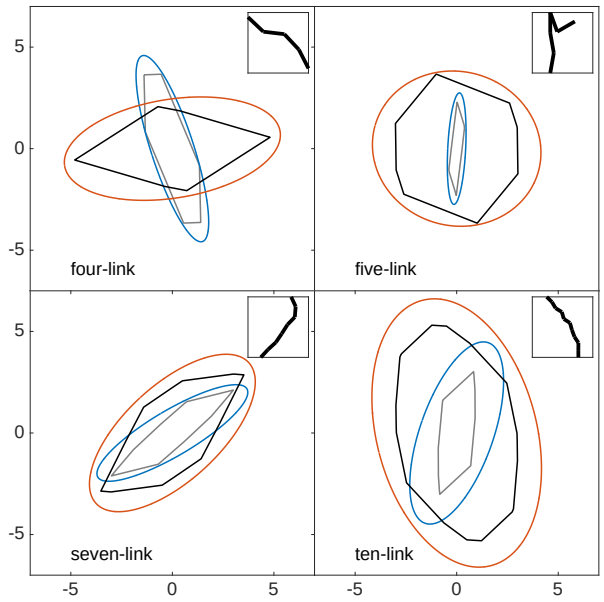

Figure 1: Feasible CoM acceleration polygons due to torque limits and CoM dynamic manipulability ellipses for four different planar robots. The black polygons and red ellipses are for constrained end-effectors whereas the grey polygons and blue ellipses are for unconstrained robots at the same configuration. The gravity and velocity are assumed to be zero ($\ddot{\mathbf{c}}_{vg} = 0$).

(iv) ten links which are connected to each other by active revolute joints. The first link of each robot is fixed to the ground by a passive revolute joint. Each link is assumed to have unit mass and length and its CoM in the middle. Corresponding robots configurations, which are chosen randomly, are depicted in the top right corner of each plot. Areas of feasible CoM accelerations (due to saturation limits) for these robots are indicated in Fig. 1 by grey and black polygons. These polygons are obtained numerically by mapping points inside the range of available joint torques ($|\boldsymbol{\tau}_i| \leq \boldsymbol{\tau}_{i_{max}}$) to the CoM acceleration space. This mapping is done by using (3). Both polygons for each robot are for a same configuration. The difference is that the black one shows the achievable area when the end point of the last link is fixed (i.e. an extra bilateral constraint). This is to show the effect of an additional constraint on feasible CoM accelerations (and also on ellipses). The extra constraint deforms the feasible area due to (i) the additional kinematic constraint limiting the movements of the CoM in some directions, and (ii) contact forces provide additional torques in some directions. Corresponding manipulability ellipses, which are calculated by using the weighting matrix in (4), are also shown in Fig. 1. Red and blue ellipses are related to constrained and unconstrained last links, respectively. Comparing the ellipses and polygons, it can be seen that, by employing (4) as a weighting matrix, these ellipses can provide reasonable approximations of achievable CoM accelerations. It is obvious that calculating ellipses is computationally much more efficient rather than obtaining polygons. Ellipses also provide analytical metrics which can be used to study and optimize a robot's physical ability to manipulate its CoM.

Including gravity and velocity to the above examples will only change center points of the polygons and ellipses and will have no effect on shapes and sizes of those areas. As an example, we consider the five-link robot in the same configuration and same torque limits as we had

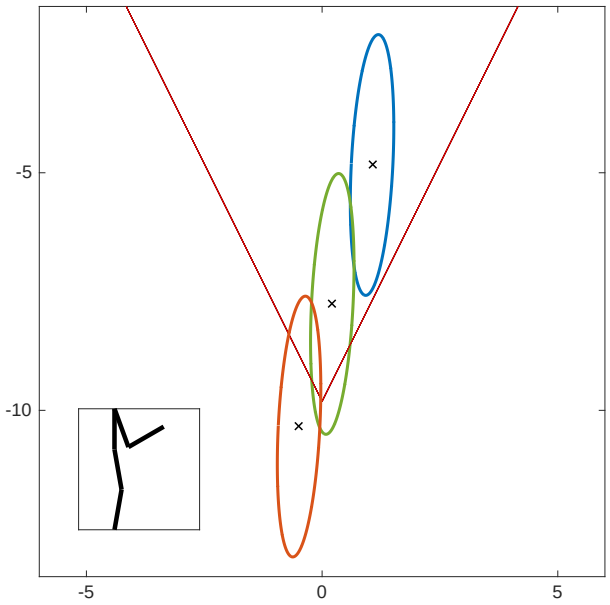

Figure 2: CoM dynamic manipulability ellipses for a five-link planar robot in different velocities. The robot's configuration is shown on the bottom left corner. Straight lines show the friction cone of the contact force.

for the ellipses in the top right corner of Fig. 1. The robot's configuration is shown in the bottom left corner of Fig. 2. The blue ellipse in this figure is the CoM manipulability ellipse for this robot when the gravity exists and velocity is zero. Therefore, the difference between this ellipse and the blue one in the top right corner of Fig. 1 is due to the gravity which only moves the center point ($\ddot{\mathbf{c}}_{vg} \neq 0$). The red and green ellipses in Fig. 2 are also for the same robot and same configuration but different velocities. This implies a kind of decoupling between the effects of inertial parameters and configuration (size and shape of the ellipse) on one hand and velocity (location of the ellipse) on the other hand. This decoupling is important in studying physical ability of a robot in different configurations independent of its velocity.

The inequality (2) for the CoM dynamic manipulability ellipsoid is derived assuming that the contacts are bilateral. Although in legged robots the contacts are usually unilateral, it is desired to maintain the contacts (except contact switching) and prevent sliding or loss of contact during the robot's performance. Therefore, bilateral contact assumption still makes sense if the contact forces satisfy the unilateral contact constraints. In the example in Fig. 2, replacing the bilateral constraint by a unilateral one in the first link, we can draw friction cone constraints in the CoM acceleration space. Straight lines in Fig. 2 show the CoM acceleration limits due to the friction cone when the coefficient of friction is 0.5. As can be seen in this figure, different velocities result in different feasible areas for a same manipulability ellipse due to the unilateral constraint. It implies that, although the CoM dynamic manipulability ellipse, which is an approximation of the robot's physical ability to accelerate its CoM, remains the same, enabling the robot to exploit that ability is dependent on velocity, as well. Note that, a proper velocity has to be determined by a controller (or a motion planner) in order to exploit available ability of a robot to reach a certain acceleration of the CoM and satisfy the contact conditions.

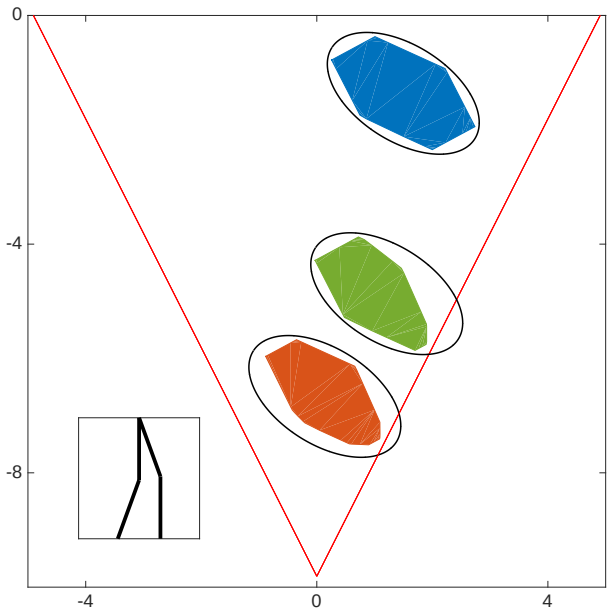

Figure 3: CoM dynamic manipulability ellipses and feasible CoM acceleration polygons due to torque limits and unilateral constraints of a four-link robot with two contact points in different velocities. Straight lines show the friction cone of the total force.

In the examples in Fig. 2, we assumed a unilateral constraint at the first link of the robot which is the same situation that arises in single support phase for legged robots. Since we also assumed that the first joint is unactuated, the CoP (and also the ZMP) is always at the contact point no matter if the robot is in balance or not. This clarifies the difference between the CoP (or the ZMP) and manipulability ellipses. As can be seen in Fig. 2, ellipses provide information about the robot's ability to accelerate the CoM in different directions with different configurations and velocities, whereas the CoP (or the ZMP) remains at the same point regardless of the robot's states.

It is worth mentioning that a larger ellipse means not only higher physical ability to accelerate the CoM, but also larger feasible region for $\ddot{\mathbf{c}}_{vg}$ to include a desired point in the CoM acceleration space inside the ellipse. In other words, although the ellipse's position and therefore its feasible part due to the unilateral constraint is dependent on $\ddot{\mathbf{c}}_{vg}$, having a larger ellipse provides more options for the controller (or the planner) to choose a proper velocity to reach a desired CoM acceleration.

Introducing more unilateral constraints to the robot (e.g. double support phase in legged robots), or having multiple contacts which at least one of them is unilateral, will result in velocity dependent limits for the CoM acceleration. In this case, each contact has its own friction cone limits which are dependent on robot's states. This is due to the relationship between contact forces and robot's velocity. Fig. 3 shows manipulability ellipses and their corresponding feasible CoM acceleration areas of a four-link robot in three different velocities. The polygons are obtained numerically and by using (3). The robot's configuration is depicted in the bottom left corner of the graph and it is chosen to mimic double support phase of a planar biped. The blue (top) area shows the feasible area when the velocity is zero and the two others are for randomly chosen velocities. By comparing the three areas, it is obvious that

different limits are affecting feasible areas at different velocities which shows the dependency of the limits on the robot's velocity.

As can be seen in Fig. 3, manipulability ellipses are the same for all velocities implying that the robot's physical ability to accelerate its CoM does not depend on velocity. However, the robot's velocity affects the feasibility of the areas due to the unilateral contacts. In other words, in all three velocities, the robot's physical ability to accelerate its CoM is the same, although in two of the velocities (i.e. green and red areas) the robot may lose its contact with the ground if it wants to reach certain accelerations. Therefore, exploiting robot's ability in a certain configuration depends on choosing proper velocity by the controller (or planner), as well. Note that, straight lines in Fig. 3 show the friction cone limits for the total contact force which do not have any effect on feasible areas at the chosen velocities since the areas are already limited by friction cone constraints of individual contact forces.

Second Choice: Joint Accelerations

Other than joint torques, joint accelerations are also important factors in studying a robot's physical ability. Obviously, producing less accelerations at the joints, with same amount of joint torques and same CoM acceleration, is desirable since it leads to lower joint velocities and consequently less joint movements. Less movements at the joints is beneficial since the robot's workspace is limited. Also lower joint velocities with same joint torques means less work and higher energy efficiency. Therefore, we introduce a proper weighting matrix in order to study the robot's CoM acceleration due to the limited joint accelerations.

Let $\mathbf{W}_q \in \mathcal{R}^{n\times n}$ denote a symmetric positive definite matrix. We define the second choice of $\mathbf{W}_\tau$ as

$$\mathbf{W}_\tau = \mathbf{J}_q^T \mathbf{W}_q \mathbf{J}_q \,. \tag{6}$$

By substituting (6) into (1), we will have

$$\boldsymbol{\tau}^T \mathbf{W}_\tau \boldsymbol{\tau} = 1 = \boldsymbol{\tau}^T \mathbf{J}_q^T \mathbf{W}_q \mathbf{J}_q \boldsymbol{\tau} \,. \tag{7}$$

Given that $\ddot{\mathbf{q}} = \mathbf{J}_q \boldsymbol{\tau} + \ddot{\mathbf{q}}_{vg}$, the above equation becomes

$$(\ddot{\mathbf{q}} - \ddot{\mathbf{q}}_{vg})^T \mathbf{W}_q \, (\ddot{\mathbf{q}} - \ddot{\mathbf{q}}_{vg}) = 1 \,, \tag{8}$$

where $\mathbf{W}_q$ can be used to unify the units or express the relative importance of the joint accelerations in $\ddot{\mathbf{q}}$. $\mathbf{J}_q$ is a Jacobian that maps joint torques to the joint acceleration and $\ddot{\mathbf{q}}_{vg}$ is a part of the joint accelerations due to gravity and joint velocities. The above equation specifies a n-dimensional ellipsoid in the joint acceleration space which its center point is at $\ddot{\mathbf{q}}_{vg}$. This point is the same center point of a n-dimensional ellipsoid that will be obtained if we project the unit weighted norm of joint torques (i.e. Eq. (1)) to the joint acceleration space. Such ellipsoid will be the same as (2) if we replace $\mathbf{J}_\tau$ with $\mathbf{J}_q$ and $\ddot{\mathbf{c}}$ with $\ddot{\mathbf{q}}$.

By choosing $\mathbf{W}_\tau$ as in (6), CoM dynamic manipulability ellipsoid will show an area in the CoM acceleration space which is achievable via unit weighted norm of joint accelerations in (8). Therefore, by setting proper values for $\mathbf{W}_q$ (user's choice based on the application), a user can study the effect of joint accelerations on reaching desired CoM accelerations. As an illustrative example, Fig. 4 shows CoM manipulability ellipses for a five-link planar robot (i.e. the same robot explained earlier in this section) in two different configurations which are shown in bottom left corners of the plots. Without losing generality, we set the gravity and velocity

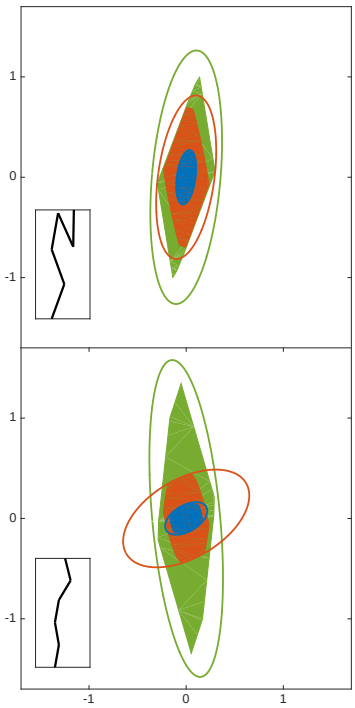

Figure 4: CoM dynamic manipulability ellipses with different weighting matrices for a planar five-link robot in two configurations. Green areas show feasible CoM accelerations due to torque limits. Blue and red areas show achievable CoM accelerations with unit weighted norms of joint accelerations.

to zero in these examples (i.e. $\ddot{\mathbf{q}}_{vg} = \ddot{\mathbf{c}}_{vg} = 0$). Torque limits for all four actuated joints are assumed to be one. Green areas show feasible CoM accelerations due to the torque limits and green ellipses are their approximations which are obtained by using (4). Blue and red areas indicate CoM accelerations which are achievable by limited norm of the joint accelerations. For the blue areas the norm is one (i.e. $\ddot{\mathbf{q}}^T\ddot{\mathbf{q}} = 1$) and for the red ones the norm is 3 (i.e. $\ddot{\mathbf{q}}^T\ddot{\mathbf{q}} = 9$). Blue and red ellipses are obtained by using (6) and setting $\mathbf{W}_q$ to identity and $1/9$ times identity matrices, respectively, to match the corresponding areas. Green, blue and red areas are obtained numerically and by using (3). In obtaining red and blue areas corresponding joint acceleration limits (i.e. $\ddot{\mathbf{q}}^T\ddot{\mathbf{q}} \leq 1$ for red areas and $\ddot{\mathbf{q}}^T\ddot{\mathbf{q}} \leq 9$ for blue areas) are also considered.

As it is expected, and also can be seen in Fig. 4, blue and red ellipses include all points in the blue and red areas, respectively. Although they also include points which are not inside their corresponding areas. The reason is that the mapping from the joint acceleration space to the CoM acceleration space is not one-to-one, which means that the mapping from the CoM to the joint acceleration space may be different. Comparing the two examples in Fig. 4, it is obvious that in the top configuration, although the green area is smaller, the blue and red areas are larger compared to the bottom plot. It means that, the same CoM accelerations can be achieved by generating smaller accelerations at the joints in the top configuration comparing with the bottom one. This can be explained by CoM dynamic manipulability ellipses as the blue and red ellipses are much more aligned with the green one in the top plot rather than in

the bottom one. Note that, blue and red ellipses have the exact same alignments and the only difference is in their sizes. Therefore, in order to minimize the norm of the joint accelerations to reach a certain CoM acceleration, one can minimize the difference in the alignments of these two ellipses.

Since the proposed metric studies the motion of the CoM, which is the main focus in balancing motions of robots, it can be used to evaluate a robot's ability to balance. Thus, we define *physical ability to balance* as a robot's physical ability to manipulate its CoM in the horizontal directions. Therefore, if we project dynamic manipulability ellipsoids of a robot, in different configurations, onto the horizontal plane, the configuration with the largest ellipse (i.e. projected ellipsoid) will have the highest ability to balance in the sense of the required torque if we use (4) or the required joint accelerations if we use (6) . Note that, the largest projected ellipse is not necessarily the projection from the largest ellipsoid, since the largest ellipsoid might be extended in another (i.e. the vertical) direction. Therefore, by using the CoM dynamic manipulability one can compare different configurations of a robot] or even different robots in terms of their physical abilities to maintain balance.

Human learning compliant force dynamics through physical interactions To explore the mechanism of human force perception has a key role in the CoDyCo project, aiming to provide natural and stable control for a humanoid robot in the similar manner with humans. Through this work,,an experimental design has been developed, and a series of human subject experiments examined the anticipated goal-directed behaviour interacting with different compliant force dynamics. Three different types of forces (a simple linear and two non-linear forces) were generated by a haptic device, and the human movements were measured against the compliant forces.The participants were asked to set the half-position andhalf-force after the certain repetitive movements to reach the target. The results showed that although humans were more sensitive to the position control than the force, they could differentiate the three dynamics. Interestingly humans seem to be more sensitive to the total power to the target than the point-force at the target.Moreover, the learning performance was also analysed and the learning curves were different between the three, suggesting some relations might exist in everyday real activities. As such, the work has deepened the understanding how humans perceive the force to reach anticipated goals ruled by the certain dynamics. This would be beneficial to apply it for providing not only natural human-robot interaction but also stable humanoid robot control when interacting with multiple compliant surfaces.

The study about human force perception and learning through compliant contact dynamics helps to design and develop a more natural and dynamical contact to humanoid robots. To explore the human learning compliant force dynamics through physical interactions, we generated four different compliant forces (two linear and two non-linear cases) by changing the stiffness values (See Figure 5).

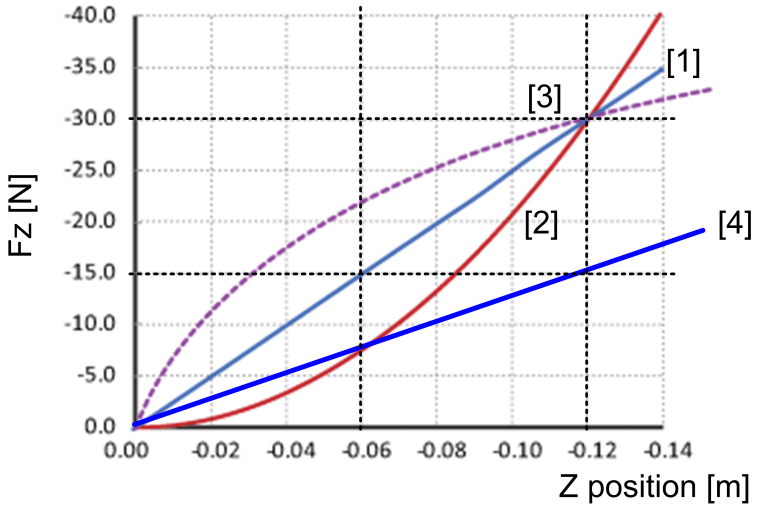

Figure 5: Four different force dynamics are applied. [1] Linear, [2] Non-linear (quadratic), [3] Non-linear (concave), and [4] Half-linear. The [1],[2],[3] are the same force at the end position (e.g., z=-0.12), and [2] and [4] are the same force at the half position (e.g., z=-0.06).

The stiffness values were calibrated depending on the goal position and the maximum force to be applied at this set position. The participants were asked to set the half-position and half-force after a certain repetition in order to be probed their responses whether or not they properly perceived the force dynamics. Figure 6 shows that although the performance tended to overshoot at both test trial due to the deprivation of the visual information of the target, the participants set the half-position in the similar manner regardless of the force dynamics. Conversely, there were significant differences between the three conditions at the half-force test trials.

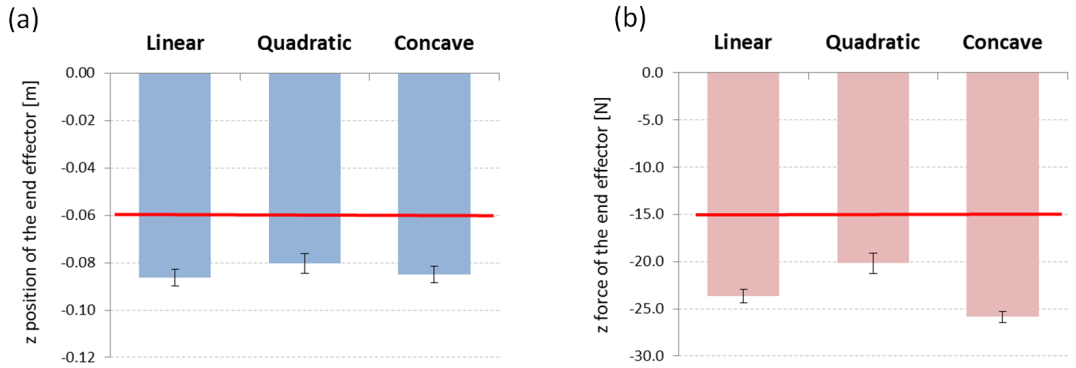

Figure 6: The test trial performances averaged across 18 participants.(a) the end-effector position at the test half-position trial and (b) the applied force at the test half-force trial. The red lines indicate the ideal values based on the dynamics (see Figure 1).

The dynamic learning evaluation revealed that there were significant differences between three forces in the learning performance averaged across 18 participants (see Figure 7). The concave force was not natural, and it was needed several repetitions to understand the dynamics and also to learn how to maintain the accuracy in reaching a target. In contrast, the linear force had less efforts but the learning model maintained a stable conditions after the repetitions. The quadratic force seemed to be a well known or natural force among the three,but still the performance gradually improved over the course of trials. These results suggest that the force model helps the user to achieve more precise and accurate movements.

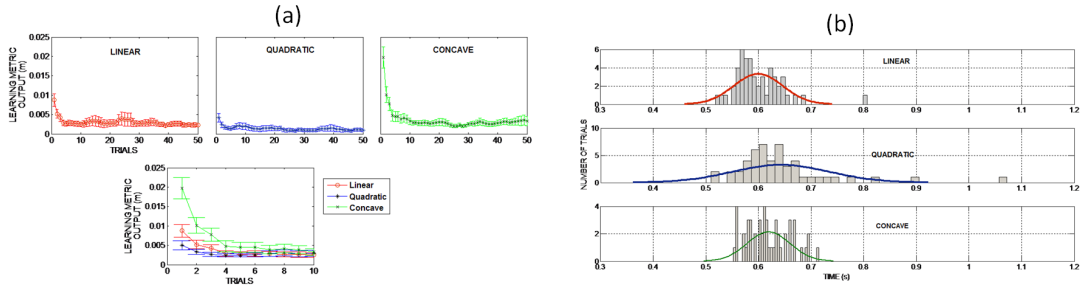

Figure 7: (a) Learning performance of the 18 participants along with the standard error. A big variation in the learning performance of the three different forces is observed within the initial 10 trials. (b) Average time taken by the 18 participants to reach the target with the three different forces.

Tactile attention and memory in multi-finger contact Given CoDyCos focus on compliant contact with support surfaces under uncertainty, an important issue is the extraction of information about the contact surfaces through the sense of touch. Knowledge about surface texture, for example, roughness which affects friction and hence contact dynamics, may be derived from static or sliding contact. Two psychology studies at UOB have examined tactile roughness through perceptual judgments and brain activation, while a third study has examined the effects of tangential load force uncertainty on precision grip cooperative lifting.

People often use several digits simultaneously to touch surfaces. Thus, they may use two fingers (eg index and middle) side by side (e.g. in steadying themselves against a stable surface) or they might use thumb opposing the index (and possibly other fingers) to form a precision grasp on either side of an object (e.g. stair rail). Often the surfaces contacted by the two digits will be the same and the double contact affords improved tactile sensitivity over single contact. However, two surfaces that are not co-located may differ in texture. For example, when using precision grip to feel fabric, the front and back surfaces may have very different textures. The perceived texture of either surface is then likely to be affected by the surface on the reverse side. We have been investigating such contact in terms of interactive effects on roughness judgments arising from simultaneous contact with two separate surfaces. Depending on the two digits involved, we have shown attention and neural cross talk afford explanations of some of the effects seen [1, 2]. Within CoDyCo we have been contrasting two forms of perceptual judgment, based on single (magnitude estimation) and two successive presentations (2-interval forced choice) of the surfaces. The theoretical interest is in the potential role of short term tactile memory in the second case. Similarity of the two digit judgments despite differences in

working memory requirements in the different perceptual tasks inclines us against a significant role for a memory component in multi-digit roughness perception. A paper is in preparation on this topic.

Surface roughness effects on brain activation in static and sliding contact Duplex theory proposes that surface roughness judgments are mediated by a combination of vibratory and spatial inputs from the slowly and rapidly adapting tactile mechanoreceptors [3]. Tactile processing by the brain primarily involves the somatosensory cortex. However, cortical areas primarily associated with auditory and visual input can also be involved. Thus, recently it has been shown that direct current stimulation of the visual or auditory cortex can facilitate spatial or temporal tactile judgments [4]. We are currently completing a brain imaging study in which we expect to demonstrate a neural basis for duplex theory. Thus we expect moving sliding textures will activate auditory cortex while static coarse textures invoke visual cortex; preliminary data in Figure 2 show auditory cortex activation with sliding contact.

The role of uncertainty in shared control of grip in cooperative lifting Social processes in cooperative multi-person action is a major topic in psychology, but there has been very little analysis of kinematics and dynamics of joint action. We have been examining control of precision grip force during a 2-person lifting task in which the load to be lifted varies from trial to trial. There are three conditions that manipulate load uncertainty. In the first condition the weight is unknown to either participant. In the second condition it is known to just one of the participants, while in the third condition it is known to both of them. We find systematic changes in anticipatory grip as a function of both ones own knowledge but also what is known by ones partner (see Figure 10).

Human arm impedance characteristics in a dynamical contact task Studies on human behaviour models with specific relation the arm movement while performaing dynamical tasks have been used to understand the prinicples behind human arm impedance[5, 6]. The effect of such impedance can be a result of the active forces (resisting or assisting) applied by the muscular reflexes, contractions and any specific joint limitations of the movement. From the literature, it is understood that the directional influence of such movements has a direct influence in the arm stiffnes or impedance specifically being anisotropic under static conditions [7]. These arm impedance characteristics have also been studied using a virtual model, while the human arm is trying to influence the virtual system by performing a dynamic task [8]. Tee et al.,[9] developed a computational model to study the effect of human arm impedance and the joint stiffness measures observed while trying to perform a task in any given dynamic enviroment (stable or unstable). These studies focus mainly on the human arm impedance models in a static or dynamic task which will help understanding the human impedance perfromance in any enviroment.

As part of the CoDyCo project, the human behaviour model while in contact with compliant forces were analysed and studied previously. Further to this analysis, it is interesting to understand the similar behaviour while in contact with a robot model or any defined object with significant dynamic influence. These intentions led to the development of the following preliminary study which is perfromed using the Haptic master along with a simulated enviroment. The goal of this task is to understand how humans emulate or modify their course of action and perception in maintaining the postural balance of a robot model.

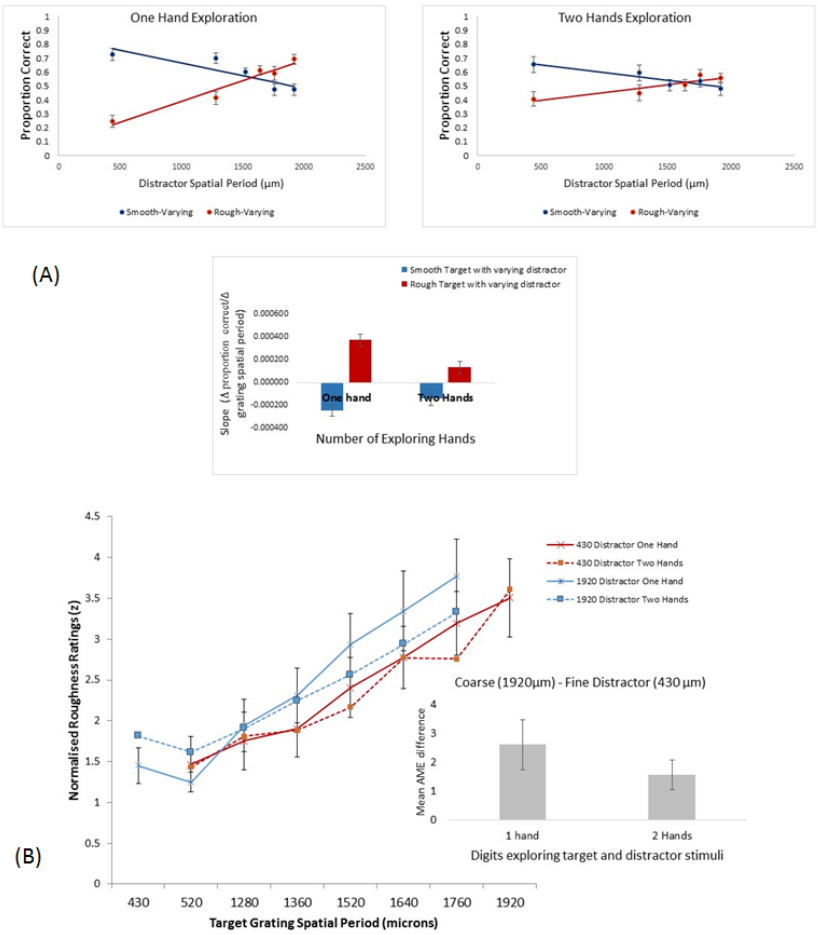

Figure 8: Multifinger contact effects on (A, above) 2-interval force choice (2-IFC) and (B, below) absolute magnitude estimates (AME) measures of roughness perception. In both tasks participants actively explored a target and distractor surface simultaneously using 2 digits; the digits were either on one hand or two hands, expected to result in more or less crosstalk. In the 2-IFC task (A), participants identified the rougher of a pair of target stimuli and were instructed to ignore the distracter. The red circles and line indicate group (N=12) average performance when the fine surfaced target was paired with various coarse distractor surfaces; a fine distractor depresses accuracy more than a coarse distractor. The blue circles and line show behaviour with the coarse target; a coarse distractor depresses accuracy more than does a fine one. The bar graph summarising mean slope across participants shows the distraction effect is greater in the one hand condition. In the AME task (B), participants rated the roughness of target surfaces while instructed to ignore the simultaneously touched distractor. The graph at the top of figure 1b shows mean ratings for each target surface. The blue crosses and squares show mean ratings for each target surface with a coarse distractor surface. Mean ratings with a fine distractor surface are shown in red. It can be seen that a coarse distracter results in higher roughness ratings than does a fine distracter. As with 2-IFC, the distracter effects are greater with the distracter on the same hand as the target.

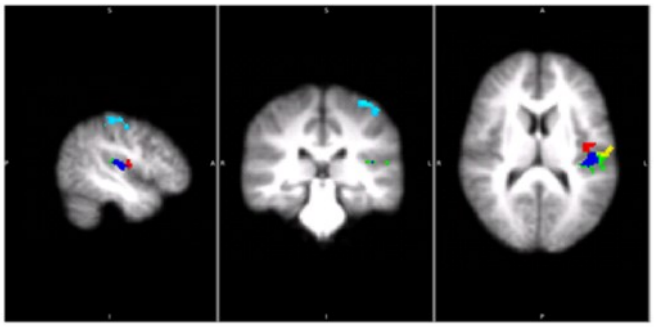

Figure 9: Activations during passive touch. The three panels indicate sagittal, coronal and horizontal planar sections of the brain with multisensory activations for a tactile discrimination task contrasting coarse and fine texture perception under moving and static touch conditions. Regions of interest shown with coloured blobs, were more activated for moving (vs static) touch, including auditory cortex (TE1.0). The stimuli were applied to the right index finger of passive participants, N=13; Light blue: BA1, Green: OP1, Red: OP3, Yellow: OP4, Blue: TE1.0

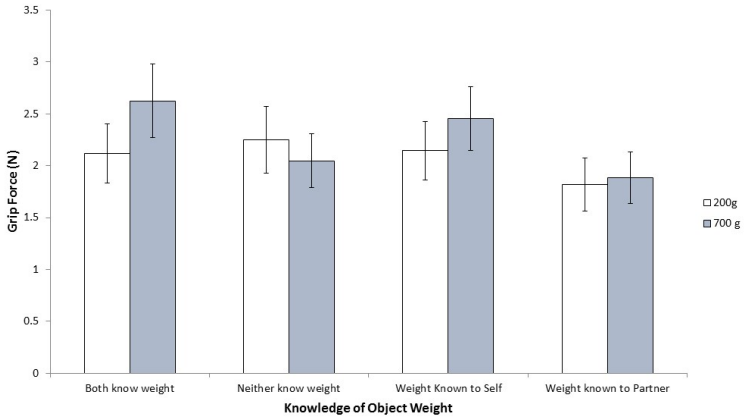

Figure 10: Joint lifting action. The participants worked in pairs to lift a bar to a target height. The weight at the centre of the bar (either 200g or 700g) was known to one, both or neither participant in pair. The force with which the participants held the bar in anticipation of a lift in the different knowledge conditions is shown along with on SE of the mean.

Methods

The human arm impedance behaviour can be studied by constraining or limiting the human movement within a specific range. Further, a dynamic task is also needed which will encourage the human to engage in continuous movement. This continuous exploration and the variation in the human arm behaviour will help in understanding the principles behind the mechanical stiffness of the human arm. Further, to answer the global objective of the CoDyCo project, we designed the dynamical task as to help or assist the humanoid robot from a sitting position to the standing position.

The robot model is designed as simple planar double inverted pendulum model which will vary its performance with respect to the velocity and the force parameters received from the Haptic master. The dynamic equation for an inverted pendulum model can be represented as

$$\ddot{x} = g/m + F_{ext}/m + F_{con}/m \tag{9}$$

F_{ext} is the external force received from the Haptic Master input and F_{con} is the controller force (PD controller) in the knee joint (to maintain the constrained movement). The force applied by the human via the Haptic Master device, is transformed directly to the end-effector position of the planar robot model. The force applied at the end effector is then transformed to the individual joint torques using the following computation:

$$\tau = J^T * F_{ext} \tag{10}$$

with τ being the joint torque to be applied in the hip, knee and ankle joints of the robot model. F_{ext} corresponds to the force applied by the human and measured through the Haptic master device.

To maintain the initial sitting position of the joints the model needs to be equipped with a PID controller or a COM based balancing controller which will further act depending on the force applied by the human through the Haptic Master.

Experimentation

The experimental setup involves the Haptic Master device which helps in emulating the human applying the necessary force to initiate the robot (model) to move from a sitting position to standing position. A planar robot model is developed using Simulink and it is directly integrated with the x and z direction forces applied by the participants. The haptic master is also limited to the planar movement which helps the human in controlling the applied moment or contact force. A real time visualization of the planar model is displayed in the monitor which helps the participant to understand and to control the arm movements.

Figure 11 presents the experimental set-up used in this analysis, the Haptic Master moog and Simulation model. Participants will visualize the pendulum model as a visual feedback and can relate the change in the movement depending on the force applied. The static (iso-metric) force model is with high stiffness emulating the body weight and the force feedback from the human is taken as a direct input.

Preliminary Results

A preliminary study was conducted to evaluate the objective of combining the dynamical task along with restricted human arm movement. This analysis help to understand the behaviour of the low level controller used in the model and influence of the human applied forces. Figure

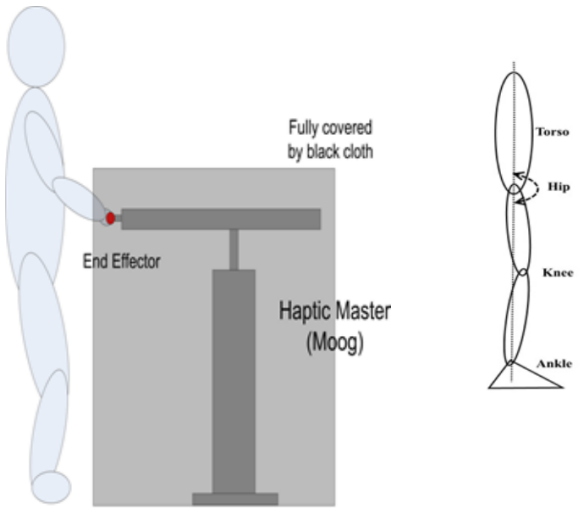

Figure 11: The spring model in the Haptic API is used to emulate the performance of a robot model (mass) and the human applies the force along the x and z directions similar to a planar movement which is visualized using the model in real time.

12 illustrates the external force observed as a result of the applied forces along the x and z axis. The participant was performing a planar motion by applying force along the x and z axis within a given free space. The forces observed to be varying continuously which signifies the dynamically exploration of the user whilst maintining a higher forces. The real time visualization of the model helped the user to increase or decrease the forces along x and z directions such as to control the movement of the planar robot model.

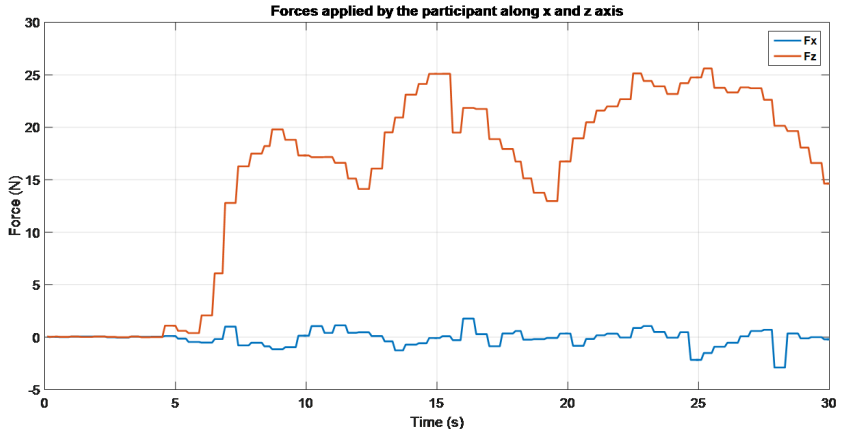

Figure 12: External forces applied by the participant along the x and z axis are measured using the Haptic Master device.

The observed torque behaviour in all the three joints of the planar model are presented in fig 13. The initial joint torques are applied based on the input from the controller which later on combines with the output from the haptic master. The torque performance explains the movement followed in the planar model, with respect to the user applied forces. The torques profile stabilises at the end of 30seconds time window which is also in relation to the stabilised

forces observed in fig. 12.

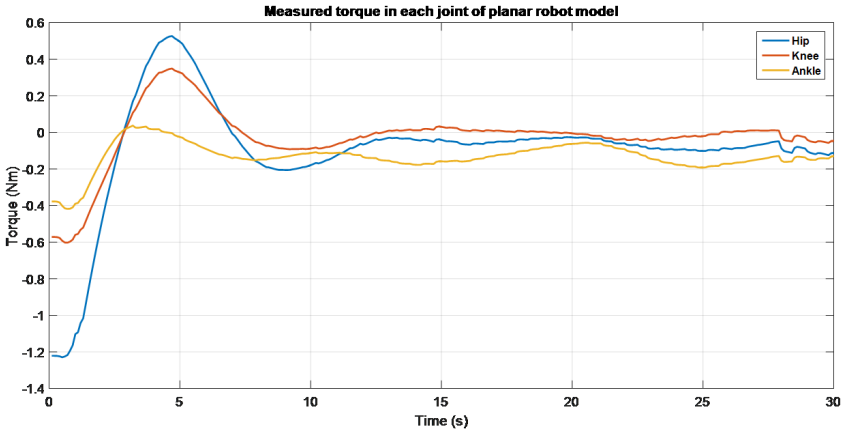

Figure 13: Resulting torque applied to the planar robot model, The torque performance varied depending on the External force applied by the user and the controller output.

Analysis of social and physical signals in human-robot interaction during assembly task We analyzed the social and physical signals exchanged by 56 human participants and the iCub during a collaborative assembly task. The experiments, performed by Serena Ivaldi at UPMC, were later analyzed during her time in TUD and INRIA. First, we focused on social signals. In [Ivaldi et al., Int. Journal of Social Robotics 2016], we reported the analysis of results concerning the influence of individual factors in gaze and speech. We found that the more an individual is extrovert, the more he/she will tend to talk to the robot; the more an individual has a negative attitude towards robot, the less he/she will gaze at the robots face and the more he/she will tend to look at the robots hands, where the physical interaction occurs. In [Anzalone et al, Int. Journal of Social Robotics 2017] we also showed that it is possible to predict the extroversion of an individual from a thin slice of face to face interaction between the human and the robot, by taking into account several movement metrics. We later started to analyze the physical signals, in particular the forces at the end-effectors of the robot (hands) where people were grasping the robot to drive and show the movement. We observed many interesting facts: the variance of median contact forces tis smaller in men than women; older people apply smaller forces; extroverts also apply small forces; by contrast, people with negative attitude towards interactions with robots (a subscale of NARS) apply bigger forces. We observed a visible difference between the demonstrations by the expert and the demonstrations provided by the participants, that were not robotics experts: the difference is highly visible, especially in terms of the variability of trajectories and different strategies adopted by the participants when moving the robot arms. Nevertheless, we observed a learning effect in the trajectories demonstrated by the participants: the smoothness of the movement, measured by the log-dimensionless jerk computed on the trajectories, increases across 3 trials in a significant way. A paper summarizing these results is currently in preparation.

Resources Overall, the use of resources within WP2 was in accordance to the plans.

WP2 person months	IIT	TUD	UPMC	UB	JSI	INRIA
Year 1	-	-	0.28	2.64	18.80	-
Year 2	-	3.00	0.48	7.67	21.85	-
Year 3	-	1.00	1.20	13.88	21.69	0.52
Year 4	-	3.00	0.56	31.50	?	1.00
Partial	?	?	?	?	?	?
Overall	-	4.00	1.00	45.00	55.00	1.00

Deviations from workplan No significant deviations.

3.3.2.3 Work package 3 progress

The progress for each task are described hereafter.

3.3.2.3.1 Reproducing existing control results in a simple case (T3.1)

The explicit goal of T3.1 for the fourth year was to ...

We achieved the following results ...

3.3.2.3.2 Formulating the control problem (T3.2)

The explicit goal of T3.2 for the fourth year was to ...

We achieved the following results ...

3.3.2.3.3 Solving the local control problem (T3.3)

The explicit goal of T3.3 for the fourth year was to ...

We achieved the following results ...

3.3.2.3.4 Bootstrapping and validating the control approach in rigid world and compliant cases (T3.4)

The explicit goal of T3.4 for the fourth year was to ...

We achieved the following results ...

3.3.2.3.5 Deviations from workplan

The PM expenses for WP3 after one year of project are globally conform to the planned one. The observed deviations are related to the fact that tasks 3.3 and 3.4 spans the overall duration of the project and the contribution of some of the partners are expected in the 2nd, 3rd and 4th year.

3.3.2.3.6 Resources

WP3 person months	IIT	TUD	UPMC	UB	JSI	INRIA
Year 1	9.90	4.60	15.15	-	-	-
Year 2	-	10.5	14.67	1.85	1.00	4.14
Year 3	-	9.65	8.79	1.63	2.00	4.03
Partial	9.90	24.75	38.61	3.48	3.00	8.17
Year 4	?	?	?	?	?	?
Partial	?	?	?	?	?	?
Overall	9.00	24.00	43.5	10.00	4.00	10.50

In order to best use the whole-body controllers developed within the framework of WP3, TUD hired a student for setting up the iCub hardware and simulation environment.

Deviations from workplan No deviations.

3.3.2.4 Work package 4 progress The progress for each task are described hereafter.

3.3.2.4.1 Generalizing and Improving Elementary Tasks with Contacts (T4.x) The explicit goal of T4.x for the fourth year was to ...

We achieved the following results ...

Resources

WP4 person months	IIT	TUD	UPMC	UB	JSI	INRIA
Year 1	-	8.00	2.22	-	-	-
Year 2	6.04	21.70	1.69	2.15	3.00	2.01
Year 3	9.79	12.00	0.74	1.68	3.00	3.30
Year 4	?	?	?	?	?	?
Partial	?	?	?	?	?	?
Overall	30.00	38.00	9.00	12.00	10.00	9.00

Deviations from workplan No deviations.

3.3.2.5 Work package 5 progress The activities in WP5 are divided into four tasks corresponding to the four years project duration. As a result, during the fourth year CoDyCo results concentrate on T5.4. The main result consist in the implementation of the validation scenario consisting of the balancing with the help of a caregiver. The main scientific contribution is described here [10].

3.3.2.5.1 Scenario 4: learning how to stand up with the help of a human caregiver (T5.4) The main contributions to T5.4 have been presented in "Validation scenario 4: learning how to stand up with the help of a human caregiver" which discusses the technical implementation of the fourth year validation scenario (see `https://github.com/robotology-playground/codyco-deliverables/tree/master/D5.4/pdf`). The software developed for the scenario implementation is released with an open-source license and distributed through github (`https://github.com/robotology/codyco`).

3.3.2.5.2 Deviations from workplan No deviations.

Resources Resources were used with no difference with respect to what planned.

WP5 person months	IIT	TUD	UPMC	UB	JSI	INRIA
Year 1	2.00	-	0.31	-	-	-
Year 2	12.00	0.85	0.05	-	-	-
Year 3	13.06	2.00	0.14	1.44	-	0.52
Year 4	?	?	?	?	?	?
Partial	?	?	?	?	?	?
Overall	48.00	5.00	2.50	-	-	1.50

Deviations from workplan No significant deviations from the workplan. The validation scenarios will include all the theoretical and technological challenges detailed in the original plan.

3.3.2.6 Work package 6 progress Activities within work package 6 achieved the expected results both in terms of administrative activities and management activities. As a major result, the software repository was consolidated thanks to the versioning tool (git) and social coding website (`https://github.com`).

3.3.2.6.1 Administrative coordination (T6.1) Administration was successfully coordinated by Chiara Andreoli at IIT. The major activity concerned an amendment that the CoDyCo consortium asked the main reason being the fact that Serena Ivaldi, initially hired by UPMC, lately moved to UPMC and finally integrated in the consortium with INRIA. Part of the administrative coordination activities were also conducted during the mid-year meeting: Nancy, November 22nd, 2016. Details on the meetings can be found in the CoDyCo website (`http://www.codyco.eu`).

3.3.2.6.2 Software repository implementation (T6.2) A github software repository was set up `https://github.com/robotology/codyco` and the contribution from the different developers can be directly checked in the website.

Resources Resources were used as follows.

WP6 person months	IIT	TUD	UPMC	UB	JSI	INRIA
Year 1	1.46	-	0.25	-	-	-
Year 2	1.50	-	0.31	-	-	-
Year 3	1.51	1.00	0.19	-	0.44	-
Year 4	?	?	?	?	?	?
Partial	?	?	?	?	?	?
Overall	5.00	1.00	1.00	0.60	1.00	-

Deviations from workplan No significant deviations.

3.3.2.7 Work package 7 progress Dissemination and exploitation activities included the participation to international events addressed to both commercial and academic institutions.

3.3.2.7.1 Dissemination activities towards academia, industry, and other users (T7.1) The explicit goal of T7.1 for the fourth year was to ...

We achieved the following results ...

3.3.2.7.2 Exploitation plan (T7.2) The explicit goal of T7.2 for the fourth year was to ...

We achieved the following results ...

3.3.2.7.3 Management of IPR (T7.3) The explicit goal of T7.3 for the fourth year was to ...

We achieved the following results ...

3.3.2.7.4 Dissemination of a database of human motion with contacts (T7.4) The explicit goal of T7.4 for the fourth year was to ...

We achieved the following results ...

Resources Resources were used as follows.

WP7 person months	IIT	TUD	UPMC	UB	JSI	INRIA
Year 1	1.00	-	0.40	-	-	-
Year 2	-	-	0.13	-	-	0.91
Year 3	1.00	-	0.11	-	-	-
Year 4	?	?	?	?	?	?
Partial	?	?	?	?	?	?
Overall	3.00	1.00	1.00	1.00	1.00	1.00

Deviations from workplan No significant deviations.

3.4 Deliverables and milestones tables

3.4.1 Deliverables (excluding the periodic and final reports)

Del. no.	Deliverable name	WP	Type	Date	Respon sible	Person Month
D1.2	Software for controlling of balancing and reaching with multiple contacts.	1	SW	M24	UB	16
D3.1	Local solver in rigid-world cases.	3	R	M24	UPMC	18
D4.2	Learning of tasks with multiple contacts by imitation and reinforcement learning.	4	R	M24	TUD	30
D5.2	Validation scenario2: balancing on feet while performing goal directed actions.	5	R	M24	IIT	13

R = Report, **P** = Prototype, **D** = Demonstrator, **SW** = Software, **O** = Other

3.4.2 Milestones

Milestone number	Milestone name	Work package(s) involved	Expected date [1]	Leader	Means of verification
MS.2	Validation scenario2: balancing on feet while performing goal directed actions	MS.1 T1.3 T1.5 T4.3 T5.2	M24	IIT	- The iCub successfully reaches an object while exploiting multiple contacts

References

[1] R. D. Roberts and G. W. Humphreys, "The role of somatotopy and body posture in the integration of texture across the fingers," *Psychological Science*, 2010.

[2] R. D. Roberts, "Roughness perception across the hands," *Attention, Perception, & Psychophysics*, vol. 75, no. 6, pp. 1306–1317, 2013.

[3] M. Hollins and S. R. Risner, "Evidence for the duplex theory of tactile texture perception," *Perception & Psychophysics*, vol. 62, no. 4, pp. 695–705, 2000. [Online]. Available: http://dx.doi.org/10.3758/BF03206916

[4] J. M. Yau, P. Celnik, S. S. Hsiao, and J. E. Desmond, "Feeling better separate pathways for targeted enhancement of spatial and temporal touch," *Psychological science*, p. 0956797613511467, 2014.

[5] M. Darainy, A. A. G. Mattar, and D. J. Ostry, "Effects of human arm impedance on dynamics learning and generalization," *Journal of Neurophysiology*, vol. 101(6), pp. 3158–3168, 2008.

[6] F. Mussa-Ivaldi, N. Hogan, and E. Bizzi, "Neural, mechanical, and geometric factors subserving arm posture in humans," *Journal of Neuroscience*, vol. 5, no. 10, pp. 2732–2743, 1985. [Online]. Available: http://www.jneurosci.org/content/5/10/2732

[7] E. Burdet, R. Osu, D. W. Franklin, T. E. Milner, and M. Kawato, "The central nervous system stabilizes unstable dynamics by learning optimal impedance," *Nature*, vol. 414, no. 6862, pp. 446–449, 2001.

[8] T. Tsuji, Y. Takeda, and Y. Tanaka, "Analysis of mechanical impedance in human arm movements using a virtual tennis system," *Biological Cybernetics*, vol. 91, no. 5, pp. 295–305, 2004. [Online]. Available: http://dx.doi.org/10.1007/s00422-004-0515-1

[9] K. P. Tee, E. Burdet, C.-M. Chew, and T. E. Milner, "A model of force and impedance in human arm movements," *Biological cybernetics*, vol. 90, no. 5, pp. 368–375, 2004.

[10] C. Latella, N. Kuppuswamy, F. Romano, S. Traversaro, and F. Nori, "Whole-body human inverse dynamics with distributed micro-accelerometers, gyros and force sensing," *Sensors*, vol. 16, no. 5, p. 727, 2016.